Unmanned aerial vehicle (UAV)-based cadastral mapping accuracy analysis: a case study of Sarayköy, Konya

Bilal Atak*1[iD], **Abdullah Varlık 2**[iD], **Ramazan Güngör 3**[iD], **Osman Salih Yılmaz 4**[iD]

1Kırşehir Ahi Evran University, Kaman Vocational School, Department of Urban Planning, Kırşehir, Türkiye,
bilal.atak@ahievran.edu.tr
2Necmettin Erbakan University, Faculty of Engineering-Architecture, Department of Topographical Engineering, Konya, Türkiye,
avarlik@erbakan.edu.tr
3Manisa Celal Bayar University, Demirci Vocational School, Department of Urban Planning, Manisa, Türkiye,
ramazan.gungor@cbu.edu.tr
4Manisa Celal Bayar University, Demirci Vocational School, Department of Urban Planning, Manisa, Türkiye,
osmansalih.yilmaz@cbu.edu.tr

Abstract

Cadastre is the process of determining and registration the geometric and legal status of real estates. The determination of the geometric status of real estates has been carried out using various methods throughout history. These methods, mostly based on local measurements, are prone to errors such as measurement, boundary, plotting, and calculation errors. These errors negatively affect project management in all engineering projects that are based on ownership today. Different solutions are being developed in cadastral applications to eliminate these negativities. Article 22/a of the Cadastral Law is one of the applications made to correct these errors. Until 2018, the delimitation of ownership was carried out with local measurements. With the update of the Large-Scale Map and Map Information Production Regulation, it can now be done with photogrammetric methods. However, this regulation leaves the details of photogrammetric products such as the number and distribution of ground control points, image processing intensity, image matching parameters, and optimization parameters to users and commercial software. This study analyzes the effect of differences in user determination, rotation parameters, image processing intensity, and optimization parameters on accuracy performance.

1. Introduction

Cadastre is a public inventory that systematically organizes property-related data, demarcating the boundaries of a country or region based on measurements [1]. Public inventories are defined as systems where each detail is represented with distinctive characteristics. Within this system, the form of property and parcel numbers are displayed on larger scaled map [2]. These maps are integrated with cadastral registration, indicating the property structure, size, value, and legal rights of all parcels [3]. In this context, cadastre provides information on the location and size of parcels by answering the questions of "where" and "how much" regarding parcels [4]. However, in past cadastral applications, errors occurred in the determination of property boundaries due to the application's form or human factors. Therefore, an amendment was made to the Cadastral Law (CL) No. 3402 on 22/02/2005 to eliminate errors arising from demarcating, measuring, drawing, and calculations. Within this scope, it was added that the renewal cadastre could be carried out in places that have undergone cadastre and titling to update the cadastral maps that have lost their application qualification, become technically insufficient,

have been found to be deficient, or do not reflect the actual boundaries on the ground, and to ensure the necessary corrections in the land registry [5].

Efforts to update cadastral registration in Türkiye involve the digitalization of cadastral boundary maps, rectification of measurement errors, completion of missing digital data, and editing of data that cannot be obtained reliably due to wear and tear [6]. To achieve this, the simultaneous execution of cadastral works related to parcels within villages and neighborhoods designated for digitalization according to Article 1 of the CL and works within the scope of Article 8 of the Temporary Provisions of the CL is expressed necessary [7]. To this end, various methods are employed to carry out the cadastral works.

In the current cadastral studies, terrestrial measurement methods such as prismatic measurement and polar measurement method and aerial photogrammetry method, which is a photogrammetric method, have been used [6]. With the aerial photogrammetry method, the General Directorate of Land Registry and Cadastre (GDLRC) produced 1/25000 scale photogrammetric maps in 1955 and 1/5000 scale maps produced from these maps were used as a basis for cadastral studies [8]. Later, with the current standards set in 1976, 1/5000 scale photogrammetric maps were actively used in cadastral studies [9].

Photogrammetry is a technique that enables measurement and drawing based on photographs [10, 11] This technique finds application in various contemporary engineering projects. Selected the Eastern Black Sea Region, which faces significant forest and agricultural land property issues, as the study area [12]. To address cadastral problems in the region, three pilot areas where cadastral surveys had not yet been conducted were identified. Subsequently, aerial photographs taken at different times for these areas were processed using digital photogrammetric methods, generating data with an accuracy of 1-1.5 meters. This data was utilized to seek solutions to the existing property problems. The spatial resolution of aerial photographs used in the resolution of property issues is very important. Nowadays, there are different aerial platforms that are used to obtain aerial photographs and produce data with very high spatial resolution.

Unmanned aerial vehicles (UAVs) have undoubtedly emerged as one of the most rapidly developing and noteworthy photogrammetric platforms in recent times [13-15]. Imagery acquired from UAV platforms finds extensive use in various military, 3D modeling, surveillance/monitoring, and mapping applications [16, 17]. UAVs combine the operational capabilities of both aerial and terrestrial photogrammetry, offering a unique set of advantages [18].

Murat et al. [19] conducted a study with a non-metric camera integrated on a UAV platform and a metric camera integrated on an airplane in 545 hectares of Derik district of Mardin province. In this context, they compared the performance analysis of the models produced from the images taken. In the analysis, the performance of the non-metric camera was tested by taking the metric camera data as reference. In this way, the accuracy of the non-metric camera integrated on the UAV platform was proved.

Altınışık [20] investigated the use of imagery acquired from a UAV platform for cadastral update works in Karaköy village, Osmancık district, Çorum province, Türkiye. The study found that the use of UAV imagery can lead to significant time and personnel savings compared to traditional ground-based surveying methods. Specifically, the study reported a 70% time saving and a 75% personnel saving. Additionally, the study found that UAV imagery can be used to accurately identify the geometric details of parcels, with an accuracy of 73.98%.

Ayyıldız [21] selected a 40-hectare area that included both residential and non- residential areas as the study area. The study involved flying at two different altitudes to obtain images with Ground Sampling Distances (GSDs) of 4 cm and 7 cm. Seven different products were generated from these images. The study found that images with a GSD of 4 cm increased image processing costs. Additionally, the study demonstrated that images with a GSD of 7 cm can be used to produce Cadastral Detail Maps (KDM) using UAV-derived imagery.

This study investigates the accuracy of UAV-derived orthophotos for cadastral update works. The study utilizes data from cadastral update works carried out in the Sarayköy neighborhood of Selçuklu district, Konya province, Türkiye. The X and Y coordinate values of detail points obtained from cadastral surveys were compared with the accuracy of 6 orthophoto images generated from UAV imagery using different parameters. Additionally, point position accuracies were examined in 4 different areas based on their proximity to the Ground Control Point (GCP) network.

2. Material and method

2.1. Study area

The study area was selected as a settlement area located within the Sarayköy neighborhood of Selçuklu district, Konya province, Türkiye, which was implemented under Article 22/a of the Cadastral Law No. 3402 (Figure 1). Sarayköy neighborhood is a neighborhood that was previously a village before the Metropolitan Municipality Law No. 6360, with 2300 cadastral parcels and an area of 2.555 hectares, 15 kilometers from the center of Konya. The cadastral survey of the parcels within the settlement area of Sarayköy neighborhood was delimited in 1976 using the prismatic measurement method. The cadastre of the parcels outside the settlement area was measured and delimited using the tachymetric measurement method. The aim of the cadastral update of Sarayköy neighborhood

was to correct the cadastral errors detected in the parcels using local measurements. The local measurement data obtained within the scope of the application were accepted as reference.
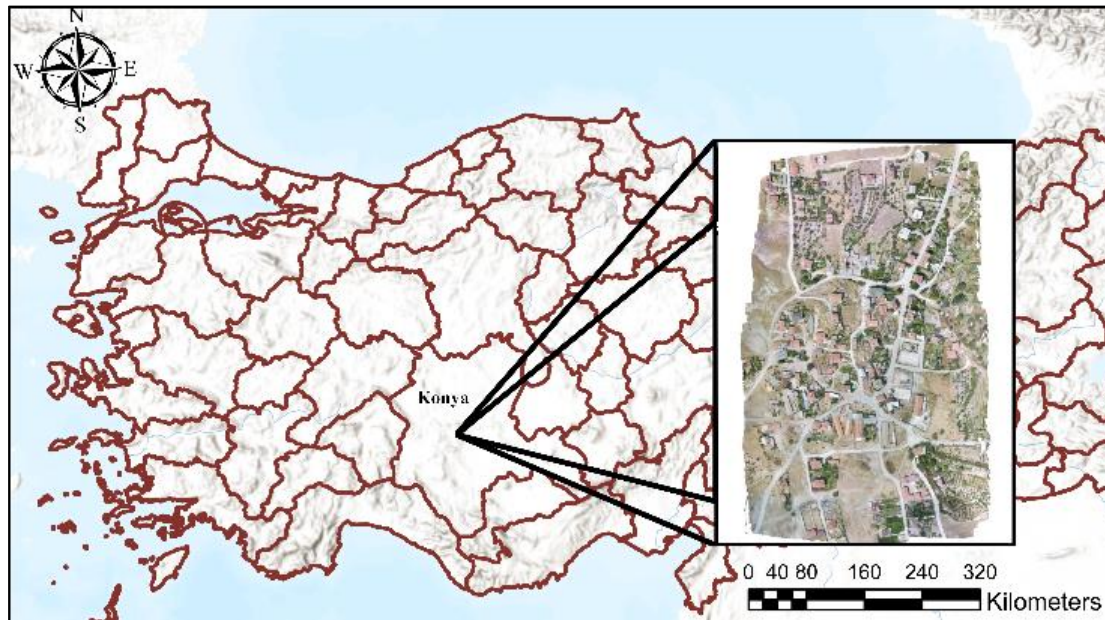

Figure 1. Study area.

2.2. Method

Maps produced by the prismatic measurement method are typically generated at scales of 1/1000 or larger for residential areas and are tied to a local coordinate system. The GCPs used in this method can be in local, cadastral, or national coordinate systems [22, 23]. Therefore, the sensitivity of the prismatic method may vary depending on the coordinate system or map scale employed. The measurement error of the prismatic method is 0.25 m, while the positional accuracy is 0.21 m at a scale of 1/500 and 0.32 m at a scale of 1/1000. The maps produced by this method are potentially considered for renewal. There are regulations that define different accuracy metrics for photogrammetric accuracy, and the values are shown in Table 1 [24].

A total of 9 Ground Control Points (GCPs) were marked within the study area. The GCPs were selected from polygons created within the scope of 22/a application and utilized for ground measurements. The measurement accuracy of these points falls within the error limit values specified by LSMMIPR. The selected polygons were marked on the ground using a template (Figure 3).

The template used to mark the GCPs on the ground consists of a 1.5x1.5 m cardboard sheet. The template was designed with 30 cm long edges, 15 cm short edges, and 10 cm gaps between them. This template was drawn on the cardboard sheet and the inner part of the cardboard was cut out. The empty areas were marked on the ground with white spray paint as shown in Figure 4.

Acquisition of aerial photographs within the study area was carried out using a DJI Phantom 3 Professional UAV with fully autonomous flight capability and a digital camera called FC 300X fixed on the UAV. The FC300X is a 12.76-megapixel non-metric camera with a 3.61mm focal length, 4000x3000 pixel resolution, and a pixel size of 1.56 μm. Image acquisition was planned using DJI's Android-based flight planning application, and two different flights were performed in the field with overlapping edges, resulting in 635 images were acquired. The flight altitude was determined as 50 meters, with overlap ratios of 80% lateral and 80% longitudinal. The acquired images were processed using Agisoft Metashape 1.7 software on a computer with Windows 64 bit, 7.91 GB RAM, Intel(R) Core(TM) i5-7400 CPU @ 3.00GHz and GeForce GT 740 features. The 9 GCPs established were used as control points and check points in the models.

The image processing software utilizes the Photogrammetric Bundle Adjustment Method to process the images and produce various photogrammetric products such as orthophotos, digital terrain models, and digital elevation models. Within the scope of this study, only orthophotos will be used. Six orthophotos with different balancing accuracies were generated by selecting different image matching parameters (yaw-pitch-roll, omega(Ω) -phi(φ)-kappa(κ)), different optimization methods (f, cx, cy and f, b1, b2, cx, cy, k1, k4, p1, p2), and different image processing densities (high, medium) provided by the software. The ground-fixed boundary lines and the parcels formed by these lines were detected from the generated orthophotos. Ground measurement data was used as reference and point position accuracy analyses were performed. The necessary checks for the map or orthophoto map scale to be produced were compared with the values specified in Articles 54, 61 and 91 of the LSMMIPR.

Table 1.Accuracy values according to different sources [24].

ASPRS, EU/JRC and LSMMIPR Comparison of Accuracy Values				
Subject	**Factor**	**ASPRS**	**EU/JRC**	**Large Scale Map and Map Information Production Regulation (LSMMIPR)**
GCP Accuracy	$RMSE_{X,Y,Z}$ -15 cm	2.5 cm	4 cm	-
Number of GCPs	Count	-	Total of 10 GCPs for one block	Total of 8 GCPs for one block
Checkpoint accuracy	GSDs -10 cm	≤± 3.33 cm	-	$V_{X,Y}$ ≤± 7.5 cm V_Z ≤± 10 cm differences ; $V_{X,Y}$max ≤± 15 cm V_{Zmax} ≤± 20 cm
Number of Checkpoint	Count	At least 20 points	At least 20 points	At least 4 GCPs and at least 30% of the total number of GCPs for a block
Matching Points Accuracy	Pixel Size-10cm	-	RMSE ≤ 5 cm	RMSE ≤ 3.33 cm
Number of Matching Points	Count	-	At least 12 points	At least 15 points
Point Position Accuracy	GSDs -10 cm	14.1 cm		14.6 cm
	GSDs -20 cm	28.3 cm	-	27.1 cm
	GSDs -30 cm	42.4 cm		44.5 cm
Point Height Accuracy	GSDs -10 cm	19.6 cm		19.4 cm
	GSDs -20 cm	39.2 cm	-	36.0 cm
	GSDs -30cm	58.8 cm		59.1 cm
DEM/DSM Grid Distance	1/1000		Scale or pixel size	10 m
	1/2000	-	5-20 times	30 m
	1/5000			30 m
Scanner Accuracy	Geometric Accuracy	-	≤± 5 µ	≤± 3 µ

RMSE:Root Mean Square Error, GCPs: Ground Control Points, MP: Matching Points,
DEM:Digital Elevation Model, DSM: Digital Surface Model

In Model 1, Ω - φ - κ was selected for image matching parameters, f, b1, b2, cx, cy, k1, k4, p1, p2 for image optimization, and high for image processing intensity. The generated model had a size of 6.73 GB and the image processing time was 16 hours.

In Model 2, Ω - φ - κ was selected for image matching parameters, f, cx, cy for image optimization, and high for image processing intensity. The generated model had a size of 7.05 GB, and the image processing time was 15 hours and 40 minutes.

In Model 3, yaw-pitch-roll was selected for image matching parameters, f, b1, b2, cx, cy, k1, k4, p1, p2 for image optimization, and high for image processing intensity. The generated model had a size of 7.04 GB and the image processing time was 19 hours and 20 minutes.

In Model 4, Ω - φ - κ was selected for image matching parameters, f, b1, b2, cx, cy, k1, k4, p1, p2 for image optimization, and medium for image processing intensity. The generated model had a size of 6.68 GB and the image processing time was 6 hours.

Study Area

⇩

Transferring aerial photographs to the system

⇩

Reference coordinate system definition

⇩

Transfer of ground control points

⇩

Sorting photos

Orientation parameter *Ω -φ-κ Image processing intensity High optimization *f, b1, b2, cx, cy, k1, k4, p1, p2	Orientation parameter *Ω -φ-κ Image processing intensity High optimization **f, cx, cy	Orientation parameter *Ω -φ-κ Image processing intensity Medium optimization *f, b1, b2, cx, cy, k1, k4, p1, p2
Orientation parameter *Yaw-Pitch-Roll Image processing intensity High optimization *f, b1, b2, cx, cy, k1, k4, p1, p2	Orientation parameter *Yaw-Pitch-Roll Image processing intensity High optimization **f, cx, cy	Orientation parameter *Yaw-Pitch-Roll Image processing intensity Medium optimization *f, b1, b2, cx, cy, k1, k4, p1, p2

⇩

Orthophoto production

⇩

Comparing the analysis results of the models

Figure 2.Workflow.

Figure 3.Ground control point marking

Figure 4.Ground control point marked with template.

In Model 5, Ω - φ - κ was selected for image matching parameters, f, cx, cy for image optimization, and medium for image processing intensity. The generated model had a size of 7.02 GB and the image processing time was 5 hours and 30 minutes.
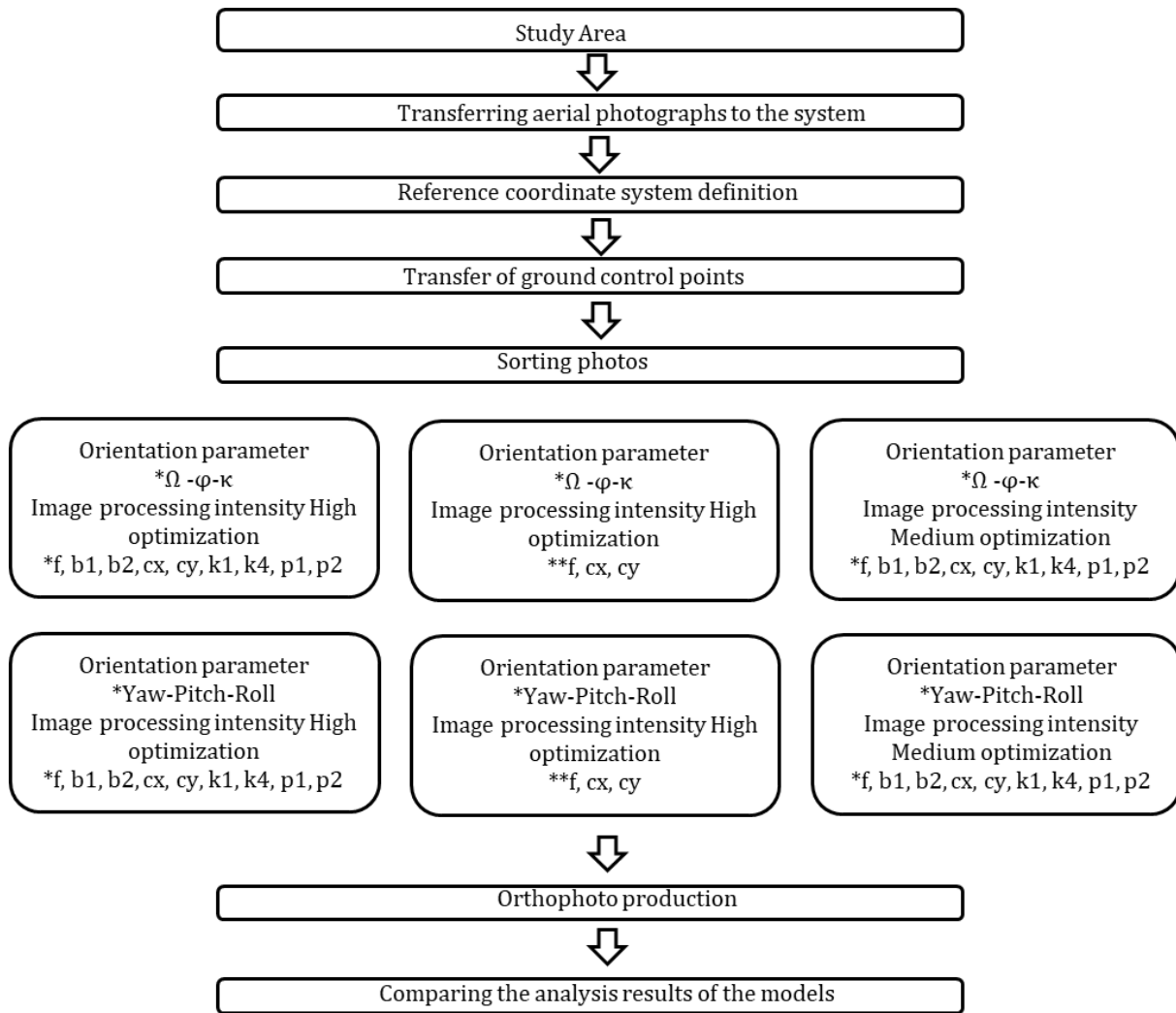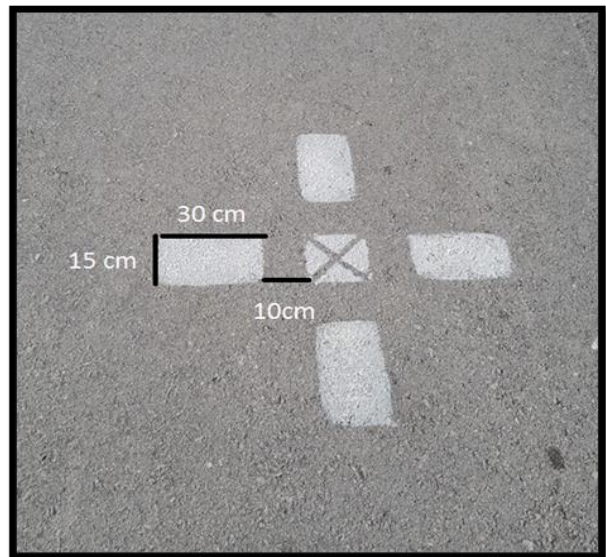
In Model 6, yaw-pitch-roll was selected for image matching parameters, f, b1, b2, cx, cy, k1, k4, p1, p2 for image

optimization, and high for image processing intensity. The generated model had a size of 7.03 GB and the image processing time was 5 hours and 30 minutes.

In the study are, fixed details identified on the model were measured using an electronic tacheometer, taking reference from polygon points also used as GCPs. This allowed for the acquisition of ground measurements of the details on the model, which were then utilized in the accuracy analysis.

3. Results

Model 1 has a ground sampling distance of 1.99 cm/px. The transformation errors of the control points (CPs) belonging to the generated orthophoto are presented in Table 2, while the transformation errors of the check points are shown in Table 3.

Table 2.CPs transformation error of model no. 1.

Label	X error (cm)	Y error (cm)
P.57347	6.87139	-0.473989
P.57352	-8.90249	-4.95934
P.57368	-0.776004	-3.38696
P.57371	-0.01861	2.64689
P.57394	1.49917	-1.11665
P.57388	-6.70631	7.71417
P.57397	6.43245	2.20801
RMSE	5.55069	3.94476

Table 3. Error check points of model no. 1.

Label	X error (cm)	Y error (cm)
P.57351	-4.47648	-2.23375
P.57396	2.60785	-2.73475
RMSE	3.66331	2.49685

Model 2 has a ground sampling distance of 1.99 cm/px. The transformation errors of the control points (CPs) belonging to the generated orthophoto are presented in Table 3, while the transformation errors of the check points are shown in Table 4.

Table 3. CPs transformation error of model no. 2.

Label	X error (m)	Y error (m)
P.57347	0.011697	0.0067762
P.57352	-0.0527766	-0.0341856
P.57368	0.00130274	-0.0500944
P.57371	0.0338416	0.00997666
P.57394	-0.0193397	0.0509574
P.57388	0.00307666	0.0994854
P.57397	0.0220169	-0.082645
RMSE	0.0265582	0.057505

Table 4. Error check points of model no. 2.

Label	X error (m)	Y error (m)
P.57351	-0.026748	0.00565044
P.57396	-0.237653	0.561141
RMSE	0.1691071	0.39680672

Model 3 has a ground sampling distance of 1.96 cm/px. The transformation errors of the control points (CPs) belonging to the generated orthophoto are presented in Table 5, while the transformation errors of the check points are shown in Table 6.

Table 5. CPs transformation error of model no. 3.

Label	X error (cm)	Y error (cm)
P.57351	2.33847	3.69604
P.57352	-1.88811	1.27837
P.57368	9.24057	-1.6866
P.57371	-0.809489	-8.83913
P.57394	5.78776	-1.1976
P.57388	-11.3698	-17.0551
P.57397	1.15048	2.54351
RMSE	6.08477	7.51236

Table 6. Error check points of model no. 3.

Label	X error (cm)	Y error (cm)
P.57347	4.76266	2.37586
P.57396	-5.78938	24.8896
RMSE	5.30093	17.6796

Model 4 has a ground sampling distance of 1.99 cm/px. The transformation errors of the control points (CPs) belonging to the generated orthophoto are presented in Table 7, while the transformation errors of the check points are shown in Table 8.

Table 7. CPs transformation error of model no. 4.

Label	X error (cm)	Y error (cm)
P.57347	1.43265	-0.856323
P.57352	-3.6727	-3.30824
P.57368	4.24217	-0.272781
P.57371	-2.59489	1.75695
P.57394	5.26311	-1.23982
P.57388	-7.91728	3.22516
P.57397	3.24245	0.721482
RMSE	4.49075	1.97478

Table 8. Error check points of model no. 4.

Label	X error (cm)	Y error (cm)
P.57351	2.81887	0.544461
P.57396	3.67279	9.87339
RMSE	3.27379	6.99215

Model 5 has a ground sampling distance of 1.97 cm/px. The transformation errors of the control points (CPs) belonging to the generated orthophoto are presented in Table 9. In model 5, all GCPs are used as control points and no check points error were produced.

Model 6 has a ground sampling distance of 1.96 cm/px. The transformation errors of the control points (CPs) belonging to the generated orthophoto are presented in Table 10, while the transformation errors of the check points are shown in Table 11.

Four distinct regions were established within the study area by taking the differences between the coordinate values of the detail points generated from the models and the coordinate values generated using the ground measurement technique, which was used as reference data. The characteristics of these regions created based on distance are shown in Table 12.

Table 9.CPs transformation error of model no. 5.

Label	X error (cm)	Y error (cm)
P.57347	1.98888	0.539777
P.57351	2.36265	2.68438
P.57352	-5.92868	-5.53369
P.57368	7.52742	-0.471951
P.57371	-0.0640455	-2.40517
P.57394	3.71021	-4.71731
P.57396	-1.1663	15.7292
P.57388	-10.293	-2.48396
P.57397	1.84962	-3.31217
RMSE	5.0094	6.06382

Table 10.CPs transformation error of model no. 6.

Label	X error (cm)	Y error (cm)
P.57347	1.95336	-0.666974
P.57352	-3.85099	-0.466929
P.57368	6.69857	-1.44323
P.57371	0.331436	-1.65623
P.57394	-2.01571	5.38178
P.57388	-6.60618	-2.64533
P.57397	3.48214	1.52597
RMSE	4.1996	2.50082

Table 11. Error check points of model no. 6.

Label	X error (cm)	Y error (cm)
P.57351	1.33356	2.19236
P.57396	8.95165	-3.279
RMSE	6.39962	2.78911

Table 12. Table of the regions determined in the study area.

Region 1	There are points 140-150 meters away from the nearest GCPs.
Region 2	There are points 80-110 meters away from the nearest GCPs.
Region 3	There are points 50-70 meters away from the nearest GCPs.
Region 4	There are points 0-40 meters away from the nearest GCPs.

4. Discussion

Upon comparing the RMSEx and RMSEy values of the 6 models generated within the scope of this study with the LSMMIPR accuracy metrics, it was determined that only Model 2 fell outside of these metrics. Additionally, it was observed that the coordinate differences generated when comparing Model 2 with the reference data increased compared to other models. It was determined that the RMSEx and RMSEy values of Model 2 remained within the regulatory error limits only when the image processing intensity was selected as medium and all GCPs were included in the transformation as control points. As a result, it was observed that the differences with the reference data decreased noticeably. Furthermore, it was observed that in Models 2 and 4, when the distance to GCPs decreased, the differences with the reference data also decreased and remained within the error limit.

When comparing Model 1 and Model 3, it was determined that Model 1 yielded more accurate results in the details of Regions I and II. It was also observed that the accuracy of the models converged as they approached the GCPs.

When comparing model 1 to model 4, it was observed that the accuracy of detail points, especially in Region I, was higher in model 1, indicating better performance. It was also found that as we approached the GCPs, the accuracies of the models were very similar to each other.

When comparing model 3 to model 6, it was observed that both models had increased accuracy as they approached the GCPs, but one model was not superior to the other.

When comparing model 1 to model 4, it was found that the accuracy performance of model 1 in every region of the study area was higher than that of model 4.

When evaluating the points individually in the study area, it was determined that point 16 in Region III was the point with the highest accuracy among the 6 models, while point 21 was identified as the point with the lowest accuracy among the models (Table 13).

Table 13. Position error of the point in each model.

Number of Point	Difference with model No. 1 (m)		Difference with model No. 2(m)		Difference with model No. 3 (m)		Difference with model No. 4(m)		Difference with model No. 5 (m)		Difference with model No. 6 (m)	
	Y	X	Y	X	Y	X	Y	X	Y	X	Y	X
1	-0.08	-0.09	-0.67	0.03	0.41	-0.04	0.28	-0.06	0.06	-0.04	0.32	-0.01
2	0.01	-0.08	-0.05	0.20	0.43	-0.08	0.45	-0.07	0.15	-0.03	0.34	-0.03
3	-0.04	-0.01	-0.41	0.23	0.46	0.11	0.35	0.07	0.18	0.12	0.43	0.13
4	0.15	-0.02	-0.35	0.06	0.66	-0.02	0.68	-0.01	0.32	-0.01	0.60	0.01
5	0.10	0.04	-0.62	0.15	0.58	0.03	0.52	0.12	0.25	0.13	0.51	0.10
6	0.09	0.07	-0.13	0.08	0.26	0.02	0.28	0.07	0.18	0.08	0.25	0.00
7	-0.21	0.07	-0.40	0.17	0.01	0.02	0.03	-0.06	-0.05	0.15	0.07	0.09
8	-0.11	0.08	-0.34	0.14	0.06	0.05	0.06	0.07	0.00	0.07	0.03	0.08
9	0.02	-0.06	-0.20	0.12	0.24	0.02	0.25	-0.04	0.13	0.03	0.18	0.03
10	-0.27	-0.21	-0.47	-0.19	-0.20	-0.20	-0.20	-0.21	-0.21	-0.16	-0.20	-0.15
11	0.00	-0.09	-0.11	0.03	0.30	-0.04	0.19	-0.06	0.16	0.04	0.22	-0.08
12	-0.11	-0.15	-0.34	-0.09	0.12	-0.18	0.04	-0.18	0.01	-0.11	-0.01	-0.15
13	0.03	-0.09	-0.22	0.01	0.15	-0.06	0.21	-0.05	0.11	0.01	0.07	-0.12
14	-0.04	-0.03	-0.22	-0.01	0.13	-0.13	0.13	-0.15	0.09	-0.08	0.19	-0.11
15	-0.10	-0.02	-0.32	0.01	0.17	0.01	0.06	-0.01	0.07	-0.01	0.11	-0.04
16	0.09	-0.03	0.09	-0.09	-0.05	-0.07	0.02	-0.07	0.04	0.01	0.04	-0.03
17	-0.02	-0.06	0.12	-0.08	-0.08	-0.20	-0.01	-0.10	-0.08	-0.14	-0.03	-0.18
18	0.03	0.07	0.09	0.12	-0.07	0.06	-0.01	0.08	-0.03	0.08	-0.06	0.05
19	-0.02	0.09	0.06	0.03	-0.05	-0.01	-0.03	-0.02	0.00	0.06	-0.10	-0.04
20	-0.10	-0.01	0.00	0.07	-0.07	0.06	0.02	0.02	-0.27	0.10	-0.04	0.03
21	-0.33	0.02	-0.34	0.04	-0.34	0.04	-0.24	-0.16	-0.3	-0.26	-0.31	-0.12

5. Conclusion

As a result of the comparison between models 2 and 4, it is concluded that an evenly distributed increase in the number of GCPs will improve the positional accuracy of the detail points. When examined in terms of image processing parameters, it was determined that the accuracy of models 1, 3, and 4 increases when Ω - φ - κ rotations are selected. Additionally, comparing models 1 and 4, it is concluded that the accuracy of the model will be within acceptable limits in every region of the study area when the image processing intensity is determined to be high. When comparing the accuracies of models 1 and 2, it was determined that optimization parameters should be selected as f, b1, b2, cx, cy, k1, k4, p1, p2 to obtain more accurate results. When examining all model comparisons, it is concluded that the most accurate results are obtained in model 1.

In future cadastral map production using photogrammetric methods, it is anticipated that accuracy will increase when models are created with stereoscopic vision.

Author contributions

Bilal Atak: Conceptualization, Data curation, Methodology, Visualization, Software.
Abdullah Varlık: Writing-Reviewing and Editing, Validation.
Ramazan Güngör: Writing-Original draft preparation, Visualization, Investigation, Writing-Reviewing and Editing.
Osman Salih Yılmaz: Visualization, Investigation, Writing-Reviewing and Editing.

Conflicts of interest

The authors declare no conflicts of interest.

References

1. Yomralıoğlu, T. (2011). Dünya'da arazi yönetimi. Türkiye'de Sürdürülebilir Arazi Yönetimi Çalıştayı. Okan Üniversitesi, İstanbul.
2. Ünel, F. B., Kuşak, L., & Yakar, M. (2022). Kamu taşınmazlarının yönetiminde değerleme. E-Kitap.
3. Güngör, R., & İnam, Ş. (2021). Value-based application in urban area design studies. Arabian Journal of Geosciences, 14(1637). https://doi.org/10.1007/s12517-021-07980-w
4. Henssen, J. (1995). Basic principles of the main cadastral systems in the world. Proceedings of the One Day Seminar Held during the Annual Meeting of Commission, 7, Cadastre and Rural Land Management, of the International Federation of Surveyors (FIG), Delft, the Netherlands.
5. Sapanoğlu, S. (2009). 3402 Sayılı kadastro kanunu, gerekçe–açıklamalar-yargıtay kararları. 1. Baskı, Ankara, Sözkesen Matbaacılık.
6. Karataş, K., & Gençer, E. (2021). Kadastro haritalarının sayısallaştırılması kapsamında yapılan çalışmaların analizi. Geomatik, 6(2), 124–134. https://doi.org/10.29128/geomatik.724163
7. Şahin, H. (2015). Kadastronun güncellenmesi, yenilenmesi ve 22a uygulamaları uygulamadaki sorunlar ve çözüm önerileri. Müfettiş yardımcılığı yetiştirme programı araştırma çalışması, Ankara.
8. Atak, B., & Durduran, S. S. (2015). Ülkemizdeki geçmiş kadastro ölçme yöntemlerinden günümüze yansıyan sorunlar ve oluşan kayıplar. WCS-CE-The World Cadastre Summit, Congress & Exhibition. İstanbul.
9. Özmüş, L., Soylu, M., Ayyıldız, E., Erkek, B., & Bakcı, S. (2016). Tapu ve Kadastro Genel Müdürlüğündeki fotogrametrik gelişmeler. Uzaktan Algılama-CBS Sempozyumu, 229-235. Adana.
10. Gu, L., Zhang, H., & Wu, X. (2024). Surveying and mapping of large-scale 3D digital topographic map based on oblique photography technology. Journal of Radiation Research and Applied Sciences, 17(1), 100772. https://doi.org/10.1016/J.JRRAS.2023.100772
11. Kanun, E., Alptekin, A., & Yakar, M. (2021). Cultural heritage modelling using UAV photogrammetric methods: a case study of Kanlıdivane archeological site. Advanced UAV, 1(1), 24–33.
12. Atasoy, M. (2004). Kadastro çalışmalarında karşılaşılan orman-mülkiyet sorunlarının çözümünde dijital fotogrametrinin uygulanması (Doğu-Karadeniz Bölgesi Örneği). Karadeniz Teknik Üniversitesi Fen Bilimleri Enstitüsü, Trabzon.
13. Colomina, I., & Molina, P. (2014). Unmanned aerial systems for photogrammetry and remote sensing: a review. ISPRS Journal of Photogrammetry and Remote Sensing, 92, 79–97. https://doi.org/10.1016/J.ISPRSJPRS.2014.02.013
14. Giordan, D., Adams, M. S., Aicardi, I., Alicandro, M., Allasia, P., Baldo, M., Berardinis, P. D., Dominici, D., Godone, D., Hobbs, P., Lechner, V., Niedzielski, T., Rotilio, M., Salvini, R., Segor, V., Sotier, B., & Troilo, F. (2020). The use of unmanned aerial vehicles (UAVs) for engineering geology applications. Bulletin of Engineering Geology and the Environment, 79, 3437-3481. https://doi.org/10.1007/s10064-020-01766-2
15. Pepe, M., Alfio, V. S., & Costantino, D. (2022). UAV platforms and the SfM-MVS approach in the 3D surveys and modelling: A review in the cultural heritage field. Applied Sciences, 12(24), 12886. https://doi.org/10.3390/app122412886
16. Ahmed, F., Mohanta, J. C., Keshari, A., & Yadav, P. S. (2022). Recent advances in unmanned aerial vehicles: a review. Arabian Journal for Science and Engineering, 47(7), 7963–7984. https://doi.org/10.1007/s13369-022-06738-0
17. Lo, L. Y., Yiu, C. H., Tang, Y., Yang, A. S., Li, B., & Wen, C. Y. (2021). Dynamic object tracking on autonomous UAV system for surveillance applications. Sensors, 21(23), 7888. https://doi.org/10.3390/s21237888
18. Güngör, R., Uzar, M., Atak, B., Yılmaz, O. S., & Gümüş, E. (2022). Orthophoto production and accuracy analysis with UAV photogrammetry. Mersin Photogrammetry Journal, 4(1), 1–6. https://doi.org/10.53093/mephoj.1122615
19. Marangoz, A. M., Karakış, S., & Numan, A. B. (2019). Geleneksel fotogrametri ile insansız hava aracı (İHA) verilerinin kullanılan kamera ve sonuç ürünleri bakımından karşılaştırılması. TMMOB Harita ve Kadastro Mühendisleri Odası, 17. Türkiye harita bilimsel ve teknik kurultayı, Ankara, Türkiye.
20. Altınışık, N. S. (2019). Kadastro güncelleme çalışmalarında insansız hava aracı (İHA)'nın kullanımının irdelenmesi: Çorum- Osmancık- Karaköy örneği. Aksaray University, Fen Bilimleri Enstitüsü.
21. Ayyıldız, E. (2020). İnsansız hava araçlarının kadastro çalışmalarında kullanımı. Türkiye Fotogrametri Dergisi, 2(1), 2932.
22. Gençer, E. (2019). Kadastrodan kaynaklı hataların düzeltilme yöntemleri. Fen Bilimleri Enstitüsü, Aksaray.
23. Günakın, Z. (2019). Türkiye'de tescil dışı kalmış yerlerin tesciline yönelik çalışmalar, karşılaşılan sorunlar ve çözüm önerileri: Çorum örneği. Aksaray University, Fen Bilimleri Enstitüsü.

24. Uysal, M., & Polat, N. (2013). Afyon Gedik Ahmet Paşa (İmaret) Camisinin fotogrametrik yöntemle üç boyutlu modellenmesi. Türkiye Ulusal Fotogrametri ve Uzaktan Algılama Birliği VII. Teknik Sempozyumu (TUFUAB'2013). Trabzon, Türkiye.